

Title	Band offset at the heterojunction interfaces of CdS/ZnSnP ₂ , ZnS/ZnSnP ₂ , and In ₂ S ₃ /ZnSnP ₂
Author(s)	Nakatsuka, Shigeru; Nose, Yoshitaro; Shirai, Yasuharu
Citation	Journal of Applied Physics (2016), 119
Issue Date	2016-05-21
URL	http://hdl.handle.net/2433/243842
Right	This article may be downloaded for personal use only. Any other use requires prior permission of the author and AIP Publishing. This article appeared in S. Nakatsuka et al., Journal of Applied Physics 119, 193107 (2016) and may be found at https://doi.org/10.1063/1.4950882 .
Type	Journal Article
Textversion	publisher

Band offset at the heterojunction interfaces of CdS/ZnSnP₂, ZnS/ZnSnP₂, and In₂S₃/ZnSnP₂

Cite as: J. Appl. Phys. **119**, 193107 (2016); <https://doi.org/10.1063/1.4950882>

Submitted: 01 March 2016 . Accepted: 06 May 2016 . Published Online: 20 May 2016

Shigeru Nakatsuka , Yoshitaro Nose, and Yasuharu Shirai



View Online



Export Citation



CrossMark

ARTICLES YOU MAY BE INTERESTED IN

[Bandgap engineering of ZnSnP₂ for high-efficiency solar cells](#)

Applied Physics Letters **100**, 251911 (2012); <https://doi.org/10.1063/1.4730375>

[First-principles study of valence band offsets at ZnSnP₂/CdS, ZnSnP₂/ZnS, and related chalcopyrite/zincblende heterointerfaces](#)

Journal of Applied Physics **114**, 043718 (2013); <https://doi.org/10.1063/1.4816784>

[Band gap of sphalerite and chalcopyrite phases of epitaxial ZnSnP₂](#)

Applied Physics Letters **96**, 231913 (2010); <https://doi.org/10.1063/1.3442917>

Journal of
Applied Physics

Special Topic:
Molecular Spintronics

Band offset at the heterojunction interfaces of CdS/ZnSnP₂, ZnS/ZnSnP₂, and In₂S₃/ZnSnP₂

Shigeru Nakatsuka, Yoshitaro Nose,^{a)} and Yasuharu Shirai

Department of Materials Science and Engineering, Kyoto University, Kyoto 606-8501, Japan

(Received 1 March 2016; accepted 6 May 2016; published online 20 May 2016)

Heterojunctions were formed between ZnSnP₂ and buffer materials, CdS, ZnS, and In₂S₃, using chemical bath deposition. The band offset was investigated by X-ray photoelectron spectroscopy based on Kraut method. The conduction band offset, ΔE_C , between ZnSnP₂ and CdS was estimated to be -1.2 eV, which significantly limits the open circuit voltage, V_{OC} . Conversely, ΔE_C at the heterojunction between ZnSnP₂ and ZnS was $+0.3$ eV, which is within the optimal offset range. In the case of In₂S₃, ΔE_C was a relatively small value, -0.2 eV, and In₂S₃ is potentially useful as a buffer layer in ZnSnP₂ solar cells. The J - V characteristics of heterojunction diodes with an Al/sulfides/ZnSnP₂ bulk/Mo structure also suggested that ZnS and In₂S₃ are promising candidates for buffer layers in ZnSnP₂ thin film solar cells, and the band alignment is a key factor for the higher efficiency of solar cells with heterojunctions. *Published by AIP Publishing.*

[<http://dx.doi.org/10.1063/1.4950882>]

I. INTRODUCTION

To date, various types of solar cells based on semiconductors with a chalcopyrite structure have been extensively investigated. Among them, CuIn_{1-x}Ga_xSe₂ (CIGS) based solar cells have achieved a high conversion efficiency of 22.3%.¹ However, CIGS contains rare elements such as In and Ga, which limits the widespread use of this material. As a result, solar absorbing materials composed of earth-abundant elements have been pursued and Cu₂ZnSnS_{4-x}Se_x solar cells have been prepared with a conversion efficiency of 12.6%.²

ZnSnP₂ is also a promising candidate as a sustainable solar absorber. According to the previous work based on bulk crystals, ZnSnP₂ with a chalcopyrite structure shows a p-type conduction with a carrier concentration of 10^{16} – 10^{18} cm⁻³ (Refs. 3–10) and has a direct bandgap of about 1.6 eV.^{8–10} In addition, a high absorption coefficient of about 10^5 cm⁻¹ in the visible light region has been reported.^{11,12} Although ZnSnP₂ thin films have been fabricated using several methods such as co-evaporation,^{11,13,14} chemical vapor deposition,¹⁵ liquid phase epitaxy,^{16,17} molecular beam epitaxy,^{18–20} and phosphidation,²¹ solar cells based on ZnSnP₂ have not been investigated.

To obtain ZnSnP₂ thin film solar cells with high conversion efficiency, band alignment between the absorber and the buffer layer is essential. Minemoto *et al.* reported that the optimal range of the conduction band offset, ΔE_C , is between 0 and $+0.4$ eV, as determined by device simulation studies of CIGS solar cells.²² When ΔE_C is larger than $+0.4$ eV, a “spike” at the interface suppresses the short circuit current density, J_{SC} . Conversely, a negative offset results in the formation of a “cliff” and limits the open circuit voltage, V_{OC} . Liu and Sites also reported that a ΔE_C from -0.4 to $+0.4$ eV

showed a high efficiency in solar cells based on CuInSe₂; the maximum efficiency was achieved when ΔE_C was -0.2 eV.²³ In addition, their simulation studies suggest that the band alignment should be flat when a Cu-poor phase, CuIn₃Se₅, exists at the interface between the buffer layer and the absorber.

As mentioned above, the selection of optimal buffer materials is important from the viewpoint of the band offset at the heterojunction interface. The experimental determination of the band offset at the interface has been reported using several methods including X-ray photoelectron spectroscopy (XPS)^{24–26} and the combination of ultraviolet photoelectron spectroscopy (UPS) and inverse photoemission spectroscopy (IPES).^{27,28} Hinuma *et al.* reported that ΔE_C of CdS/ZnSnP₂ and ZnS/ZnSnP₂ is approximately -0.2 and $+1.0$ eV, respectively, based on a first-principles study.²⁹ However, the experimental determination of the band offset between the ZnSnP₂ and the buffer layers has not been investigated. In particular, buffer layers are generally prepared by a solution process and it may be much different with the structure considered in calculation. Therefore, in this study, the band offset between ZnSnP₂ and sulfides such as CdS, ZnS, and In₂S₃ was experimentally evaluated using XPS. In addition, we investigated the current density–voltage (J - V) curves of the heterojunction diodes to determine the influence of the band offset on the J - V characteristics.

II. EXPERIMENTAL METHODS

The heterojunctions of sulfides/ZnSnP₂ were fabricated on the ZnSnP₂ bulk crystals with a diameter of 5 mm and a thickness of 0.5 mm. The crystal growth of ZnSnP₂ was performed by the flux method according to our previous work.¹⁰ Raw materials such as Zn shots (99.99%, Kojundo Chemical Laboratory), Sn shots (99.99%, Kojundo Chemical Laboratory), and red phosphorus flakes (99.9999%, Kojundo Chemical Laboratory) were sealed in

^{a)} Author to whom correspondence should be addressed. Electronic mail: nose.yoshitaro.5e@kyoto-u.ac.jp. Tel.: +81-75-753-5472. Fax: +81-75-753-3579.

TABLE I. The experimental conditions for chemical bath deposition of CdS, ZnS, and In_2S_3 thin films. TU: Thiourea ($\text{CS}(\text{NH}_2)_2$), TAA: Thioacetamide (CH_3CSNH_2), EDTA: Ethylenediaminetetraacetic acid ($[\text{CH}_2\text{N}(\text{CH}_2\text{COOH})_2]_2$), and AcOH: Acetic acid (CH_3COOH).

Sulfide	Chemical bath composition	pH	Water bath temperature ($^\circ\text{C}$)	Deposition time (min)	Reference
CdS	Cd(CH_3COO) ₂ : 1 mM TU: 5 mM CH ₃ COONH ₄ : 10 mM NH ₃ : 0.4M	11	80	13	30
ZnS	Zn(CH_3COO) ₂ : 40 mM TAA: 0.16M EDTA: 16.5 mM	5	80	240	31
In_2S_3	$\text{In}_2(\text{SO}_4)_3$: 25 mM TAA: 0.1M AcOH: 0.1M	2	70	40	32

an evacuated quartz ampoule. The ampoule was then placed in the growth furnace and heated up to 700°C and an unidirectional solidification was performed from the bottom with a cooling rate of $0.7^\circ\text{C}/\text{h}$. After the crystal growth, ZnSnP_2 bulk crystals were cut into wafers by a diamond wheel and the surface of the wafers was mechanically polished with a series of emery papers and finally with a $1\ \mu\text{m}$ diamond slurry on a buffing sheet. The CdS,³⁰ ZnS,³¹ and In_2S_3 ³² films were deposited on the ZnSnP_2 wafers using the chemical bath deposition (CBD) method. The experimental details of the CBD method are summarized in Table I. The interfaces of the sulfides/ ZnSnP_2 were analysed by scanning transmission electron microscopy (STEM, JEM-2100F, JEOL) with energy dispersive X-ray (EDX). The XPS (JPS-9010TRX, JEOL) measurements were conducted at a pressure below 10^{-6} Pa. A monochromatic Al K α (1486.7 eV) was used as an incident X-ray. In these

measurements, we evaluated the P 2*p* and S 2*p* core-levels as well as the valence band maximum from ZnSnP_2 bulk crystals with and without a sulfide-coating. For the P 2*p* level, the XPS measurements were performed using the bulk ZnSnP_2 crystals after Ar-sputtering at 300 eV for 150 s to remove the surficial oxidized layer. The level of S 2*p* was obtained from the ZnSnP_2 wafer coated by each sulfide. In this case, the surface of the samples was also sputtered for 30–75 s, where the spectra from P 2*p* were not observed. After the measurements on S 2*p*, we performed additional Ar-sputtering for the sulfide-coated samples until the XPS spectra of both P 2*p* and S 2*p* were obtained to evaluate their difference at the interface of the sulfides/ ZnSnP_2 . In this study, the XPS measurements suggested that no metallic phases were obtained in the Ar-sputtered samples, although it was reported that Ar-sputtering may change the composition of the surface or form metallic phases under the severe conditions such as higher voltage and longer period.²⁷ To investigate the effect of the band offset at the heterojunction on the *J*–*V* characteristics, we fabricated the diodes with an Al/sulfides/ ZnSnP_2 bulk/Mo structure and measured the *J*–*V* curves under dark conditions. In these devices, the Al surface electrode (~ 200 nm) and Mo back electrode (~ 400 nm) were fabricated by vacuum-evaporation and sputtering, respectively.

III. RESULTS AND DISCUSSION

Figure 1 shows the STEM images and the corresponding elemental mappings of the CdS/ ZnSnP_2 , ZnS/ ZnSnP_2 , and In_2S_3 / ZnSnP_2 interfaces. The STEM images show that the CdS, ZnS, and In_2S_3 thin films were deposited on the ZnSnP_2 bulk crystals with a thickness of approximately 100, 50, and 200 nm, respectively. The energies of the characteristic X-rays of Sn, Cd, and In are similar and then it seems that

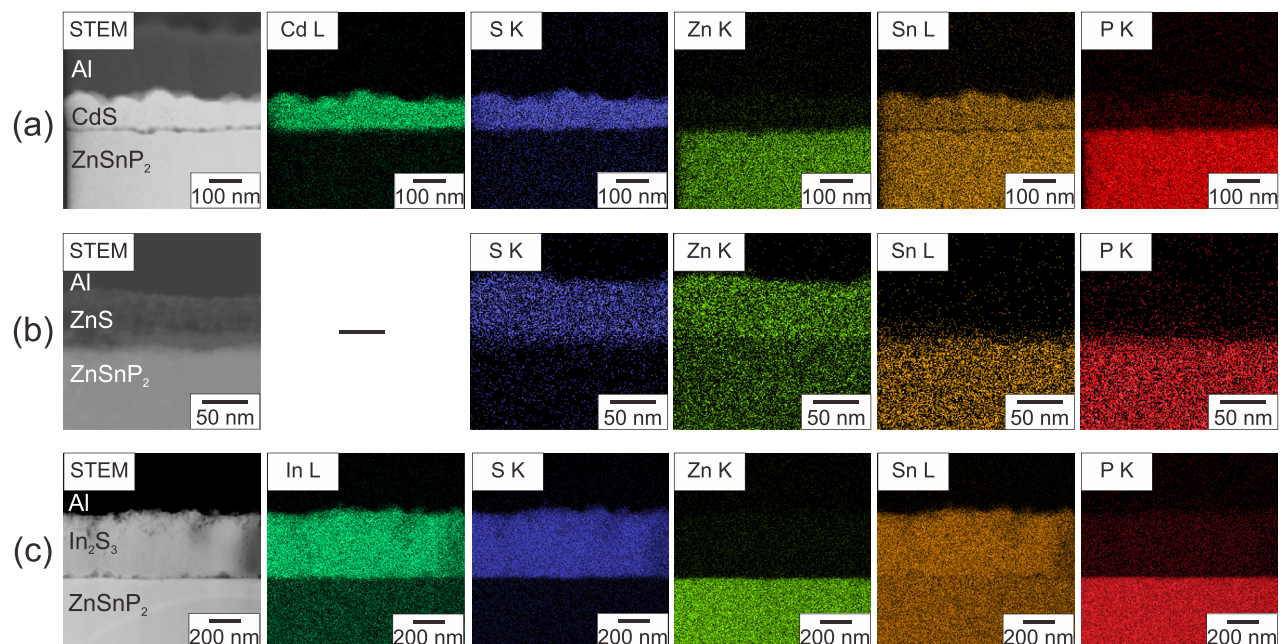


FIG. 1. The cross-sectional STEM images and corresponding EDX elemental mappings of the interfaces of (a) CdS/ ZnSnP_2 , (b) ZnS/ ZnSnP_2 , and (c) In_2S_3 / ZnSnP_2 .

TABLE II. The composition of sulfide thin films analysed by XPS spectra using the RSF method. The possible error of composition is about 10%.³⁴

Sulfide	Composition (at. %)		
	Cations (Cd, Zn, In)	S	O
CdS	51.2	34.4	14.4
ZnS	48.3	40.7	11.0
In ₂ S ₃	48.3	40.4	11.3

Sn penetrated into sulfide films. For the other elements, the interdiffusion between the sulfides and ZnSnP₂ was not remarkably observed. The surface SEM images of the sulfide-coated ZnSnP₂ and grazing incidence XRD (GI-XRD) profiles of the sulfide films are shown in the supplementary material.³³ The compositions of the sulfide films were analysed by XPS using Relative Sensitive Factor (RSF) method, in which it is known that the composition error is about 10%.³⁴ As shown in Table II, these sulfides contain a small amount of oxygen. The co-existence of sulfide and oxide and/or hydroxide is commonly observed in sulfide thin films prepared by the CBD method.³⁵ Figure 2 shows the XPS spectra of the core-levels and valence band regions of ZnSnP₂, CdS, ZnS, and In₂S₃. In these spectra, P 2*p* and S 2*p* split into 2*p*^{1/2} and 2*p*^{3/2} because of spin-orbit interactions. The XPS spectra of the core-levels at the interface between the sulfides and ZnSnP₂ are shown in Figure 3. At the interface, two peaks related to P 2*p* were observed. The peak at approximately 129 eV, observed in all samples, is derived from ZnSnP₂ because its binding energy corresponds to that of P 2*p* in GaP,³⁶ which has a similar crystal structure to ZnSnP₂. Another peak is observed at approximately 134 eV at the interfaces of CdS/ZnSnP₂ and ZnS/ZnSnP₂, which is considered to be derived from phosphate.³⁶ The peak positions of the P 2*p*^{3/2} and S 2*p*^{3/2} core-levels were determined by Gaussian fitting, and the core-level binding energies are summarized in Table III. The fitting error was less than 0.02 eV. The valence band offset at the heterojunction interface, ΔE_V , was evaluated based on the method by Kraut *et al.*³⁷

$$\Delta E_V = E_{CL-VBM}^{ZnSnP_2} - E_{CL-VBM}^{Sulfides} + \Delta E_{CL}, \quad (1)$$

where $E_{CL-VBM}^{ZnSnP_2}$ and $E_{CL-VBM}^{Sulfides}$ represent the energy differences between the core-level and the valence band maximum in ZnSnP₂ and the sulfides, respectively. ΔE_{CL} is the energy difference between the core-levels of ZnSnP₂ and the sulfides at the interface of the heterojunction. In this work, the positive value of ΔE_V indicates that the valence band maximum of the sulfides is lower than that of ZnSnP₂. The ΔE_C was calculated using the bandgaps of ZnSnP₂ and the sulfides, $E_g^{ZnSnP_2}$ and $E_g^{Sulfides}$, as shown in the following equation:

$$\Delta E_C = E_g^{Sulfides} - E_g^{ZnSnP_2} - \Delta E_V. \quad (2)$$

ΔE_C is positive when the conduction band minimum of sulfides is higher than that of ZnSnP₂. The bandgaps of CdS, ZnS, and In₂S₃ were evaluated to be 2.4, 3.8, and 2.5 eV,

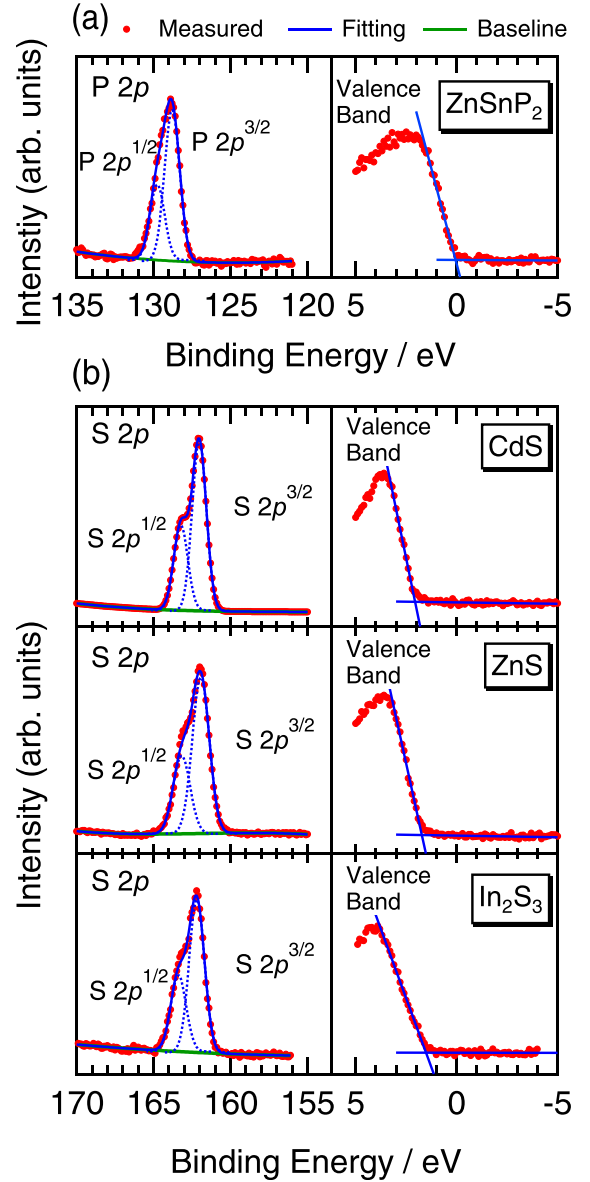


FIG. 2. The XPS spectra of the core-levels and valence band regions of (a) ZnSnP₂ and (b) sulfides. To remove the surficial oxidized layer, ZnSnP₂, CdS, ZnS, and In₂S₃ were Ar sputtered for 150, 75, 60, and 30 s, respectively.

respectively, from the transmittance of their films on glass substrates. The details of the evaluation for the bandgaps are described in the supplementary material.³³ The ΔE_C between the ZnSnP₂ and the sulfides was thus obtained as shown in Fig. 4. The ΔE_C between ZnSnP₂ and CdS, ZnS, and In₂S₃ was -1.2 , $+0.3$, and -0.2 eV, respectively. In the bandgap estimation, there might be an error of approximately 0.1 eV. Therefore, we considered that the ΔE_C also has an error of about 0.1 eV. According to the device simulations reported by Minemoto *et al.*²² and Liu and Sites,²³ it is expected that the significant ΔE_C between CdS and ZnSnP₂ leads to a small value of V_{OC} and it is difficult to achieve a higher conversion efficiency. In the case of ZnS, the ΔE_C of $+0.3$ eV is within the optimal range determined by device simulation. Thus, ZnS is considered as one of the candidates for the buffer layer in ZnSnP₂ solar cells. Hinuma *et al.* reported

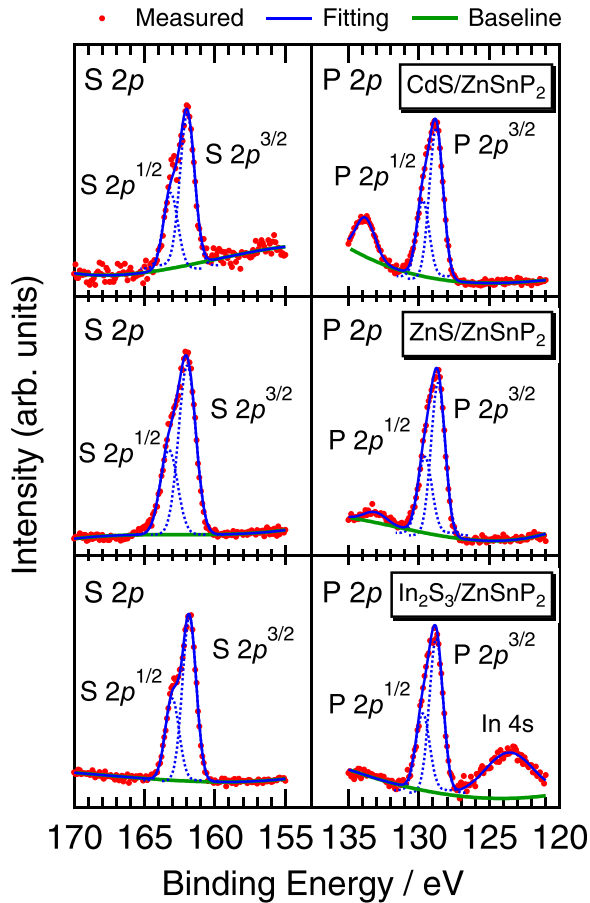


FIG. 3. The XPS spectra of the core-levels at the interface between the sulfides and ZnSnP₂. To obtain these spectra, CdS, ZnS, and In₂S₃-coated samples were Ar sputtered for 95, 120, and 350 s, respectively.

that the valence band offset at CdS/ZnSnP₂ and ZnS/ZnSnP₂ has been calculated to be 1.0 and 1.2 eV using the HSE06 hybrid functional.²⁹ A more recent theoretical study using the GWT¹ approximation has shown that quasi-particle shifts from HSE06 lower the valence bands of CdS and ZnS by 0.2 and 0.3 eV, respectively, with respect to GaP and InP.^{38,39} Assuming a similar tendency, the theoretical valence band offsets at CdS/ZnSnP₂ and ZnS/ZnSnP₂ would be about 1.2 and 1.5 eV, respectively. Considering the experimental band gaps obtained in this study, the ΔE_C at CdS/ZnSnP₂ and ZnS/ZnSnP₂ are calculated to be -0.4 and $+0.7$ eV, respectively, based on Equation (2). The discrepancies from the

TABLE III. P 2p^{3/2} and S 2p^{3/2} core-level binding energy for all samples and E_{CL-VBM} for ZnSnP₂, CdS, ZnS, and In₂S₃. ΔE_{CL} and ΔE_V were calculated from the above values.

Sample	P 2p ^{3/2} (eV)	S 2p ^{3/2} (eV)	E_{CL-VBM} (eV)	ΔE_{CL} (eV)	ΔE_V (eV)
ZnSnP ₂ bulk	128.8(0)	...	128.7(5)
CdS film	...	162.0(3)	159.9(8)
ZnS film	...	161.9(3)	160.2(1)
In ₂ S ₃ film	...	162.2(0)	160.6(8)
CdS/ZnSnP ₂	128.7(6)	161.9(6)	...	33.2(0)	2.0
ZnS/ZnSnP ₂	128.6(3)	161.9(7)	...	33.3(4)	1.9
In ₂ S ₃ /ZnSnP ₂	128.7(7)	161.8(2)	...	33.0(5)	1.1

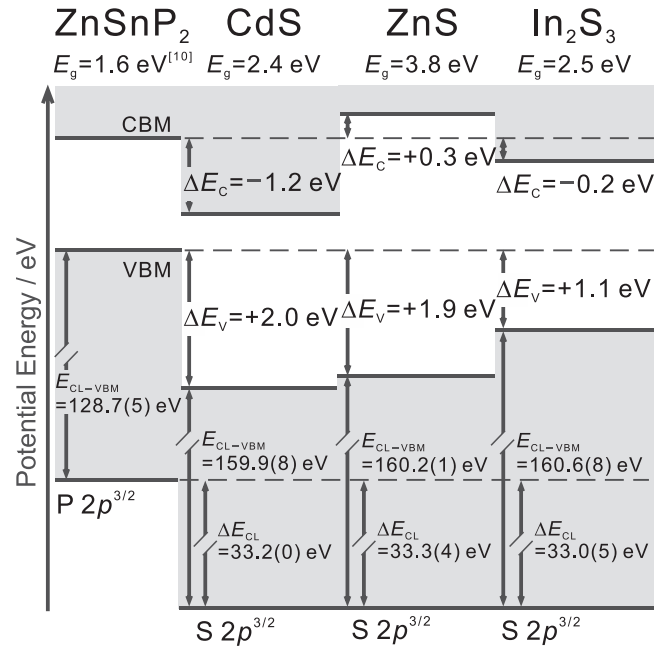


FIG. 4. Band alignment of ZnSnP₂, CdS, ZnS, and In₂S₃. The bandgap value of each compound bulk was adopted for the evaluation of ΔE_C at the interface.

experimental values of -1.2 and $+0.3$ eV are partly attributed to the differences in the orientation, atomic structure, and local chemical composition at the interfaces, all of which affect the contribution of the interfacial dipole to the band offsets. In particular, the formation of sulfide films by a solution process might affect the structure of the interfaces. Conversely, the ΔE_C at In₂S₃/ZnSnP₂, -0.2 eV, was relatively small. Therefore, In₂S₃ is potentially useful as a buffer layer.

To investigate the effect of the band offset on the heterojunction diodes, we measured the J - V curves of the diodes with an Al/sulfides/ZnSnP₂ bulk/Mo structure under dark conditions. Fig. 5 shows the J - V characteristics of the heterojunction diodes. We confirmed the ohmic contacts between the Al surface electrodes and the sulfides. The diodes using ZnS and In₂S₃ show a smaller current density than that of CdS by three orders of magnitude, which might be attributed to the high resistivities of ZnS and In₂S₃ of 4×10^7 and

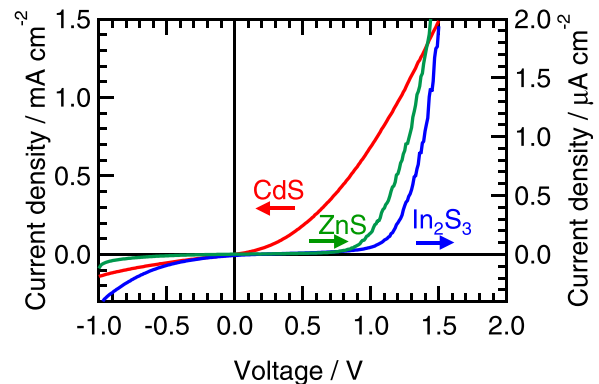


FIG. 5. J - V characteristics of the heterojunction diodes with an Al/sulfides/ZnSnP₂ bulk/Mo structure. The left axis is for CdS, and the right axis is for ZnS and In₂S₃.

$5 \times 10^6 \Omega \text{ cm}$, compared with the resistivity of CdS of $8 \times 10^2 \Omega \text{ cm}$. The resistivity measurements were performed using the films on glass substrates by the van der Pauw method under dark conditions. In the case of CdS, the current density builds up gradually, which indicates that the recombination current is dominant because the ΔE_C between CdS and ZnSnP₂ is negatively large. The small ΔE_C makes an exponential curve of current density and the turn-on voltage is more than 1.0 eV, as shown in the case of ZnS and In₂S₃. Therefore, ZnS and In₂S₃ are potentially promising materials for the buffer layer in the ZnSnP₂ solar cells. These experiments also revealed that the J - V characteristics are considerably influenced by the band offset.

IV. CONCLUSION

In this study, we evaluated the band offset of heterojunctions between ZnSnP₂ and the sulfides, CdS, ZnS, and In₂S₃, by X-ray photoelectron spectroscopy using the method reported by Kraut. The conduction band offset, ΔE_C , of CdS/ZnSnP₂ was estimated to be -1.2 eV , which forms a cliff at the interface and significantly limits the open circuit voltage, V_{OC} . Conversely, the ΔE_C of the heterojunction of ZnS/ZnSnP₂ was $+0.3 \text{ eV}$, which is within the optimal offset range suggested by device simulation studies. In the case of In₂S₃, the ΔE_C was -0.2 eV , which is a relatively small offset; therefore, In₂S₃ is potentially useful as a buffer layer in the ZnSnP₂ solar cells. The results from the turn-on voltages obtained from the J - V measurements of the sulfides/ZnSnP₂ diodes support the tendency of the band alignment, and the performance of the solar cells remarkably depends on the band offset. Therefore, ZnS and In₂S₃ are promising candidates for buffer layers in the ZnSnP₂ thin film solar cells.

ACKNOWLEDGMENTS

The authors wish to thank Dr. Y. Sonobayashi (Kyoto University) for the XPS measurements, Professor F. Oba (Tokyo Institute of Technology) for the insightful comments about the calculation of band offsets, and Professor T. Minemoto (Ritsumeikan University) and Professor S. Ikeda (Osaka University) for their help in the chemical bath deposition experiments. This work was partly supported by the JST PRESTO program, by the Elements Science and Technology Project from MEXT, and by the JSPS KAKENHI Grant No. 26289279.

¹See <http://www.solar-frontier.com/eng/news/2015/C051171.html> for Solar Frontier Archives World Record Thin-Film Solar Cell Efficiency: 22.3% (last accessed February, 2016).

²W. Wang, M. T. Winkler, O. Gunawan, T. Gokmen, T. K. Todorov, Y. Zhu, and D. B. Mitzi, *Adv. Energy Mater.* **4** (published online 2014).

³A. A. Vaipolin, N. A. Goryunova, L. I. Kleshohinskii, G. V. Loshakova, and E. O. Osmanov, *Phys. Status Solidi* **29**, 435 (1968).

⁴M. Rubenstein and R. W. Ure, *J. Phys. Chem. Solids* **29**, 551 (1968).

⁵N. A. Goryunova, F. P. Kesamanly, and G. V. Loshakova, *Sov. Phys. - Semicond.* **1**, 844 (1968).

⁶F. M. Berkovskii, D. Z. Garbuzov, N. A. Goryunova, G. V. Loshakova, S. M. Ryvkin, and G. P. Shpen'kov, *Sov. Phys. - Semicond.* **2**, 618 (1968).

⁷N. A. Goryunova, M. L. Belle, L. B. Zlatkin, G. V. Loshakova, A. S. Poplavnoi, and V. A. Chaldyshev, *Sov. Phys. - Semicond.* **2**, 1126 (1969).

⁸A. A. Abdurakhimov, L. V. Kradinova, Z. A. Parimbekov, and Y. V. Rud', *Sov. Phys. - Semicond.* **16**, 156 (1982).

⁹M. A. Ryan, M. W. Peterson, D. L. Williamson, J. S. Frey, G. E. Maciel, and B. A. Parkinson, *J. Mater. Res.* **2**, 528 (1987).

¹⁰S. Nakatsuka, H. Nakamoto, Y. Nose, T. Uda, and Y. Shirai, *Phys. Status Solidi C* **12**, 520 (2015).

¹¹H. Y. Shin and P. K. Ajmera, *Mater. Lett.* **5**, 211 (1987).

¹²T. Yokoyama, F. Oba, A. Seko, H. Hayashi, Y. Nose, and I. Tanaka, *Appl. Phys. Express* **6**, 061201 (2013).

¹³P. K. Ajmera, H. Y. Shin, and B. Zamanian, *Sol. Cells* **21**, 291 (1987).

¹⁴H. Y. Shin and P. K. Ajmera, *Mater. Lett.* **8**, 464 (1989).

¹⁵J. Sansregret, *Mater. Res. Bull.* **16**, 607 (1981).

¹⁶G. A. Davis and C. M. Wolfe, *J. Electrochem. Soc.* **130**, 1408 (1983).

¹⁷G. A. Davis, M. W. Muller, and C. M. Wolfe, *J. Cryst. Growth* **69**, 141 (1984).

¹⁸S. Francoeur, G. A. Seryogin, S. A. Nikishin, and H. Temkin, *Appl. Phys. Lett.* **74**, 3678 (1999).

¹⁹G. A. Seryogin, S. A. Nikishin, H. Temkin, A. M. Mintairov, J. L. Merz, and M. Holtz, *Appl. Phys. Lett.* **74**, 2128 (1999).

²⁰B. Lita, M. Beck, R. S. Goldman, G. A. Seryogin, S. A. Nikishin, and H. Temkin, *Appl. Phys. Lett.* **77**, 2894 (2000).

²¹S. Nakatsuka, Y. Nose, and T. Uda, *Thin Solid Films* **589**, 66 (2015).

²²T. Minemoto, T. Matsui, H. Takakura, Y. Hamakawa, T. Negami, Y. Hashimoto, T. Uenoyama, and M. Kitagawa, *Sol. Energy Mater. Sol. Cells* **67**, 83 (2001).

²³X. Liu and J. R. Sites, *AIP Conf. Proc.* **353**, 444 (1996).

²⁴Y. Hashimoto, K. Takeuchi, and K. Ito, *Appl. Phys. Lett.* **67**, 980 (1995).

²⁵Y. Okano, T. Nakada, and A. Kunioka, *Sol. Energy Mater. Sol. Cells* **50**, 105 (1998).

²⁶T. Nakada, M. Hongo, and E. Hayashi, *Thin Solid Films* **431–432**, 242 (2003).

²⁷M. Morkel, L. Weinhardt, B. Lohmüller, C. Heske, E. Umbach, W. Riedl, S. Zweigart, and F. Karg, *Appl. Phys. Lett.* **79**, 4482 (2001).

²⁸L. Weinhardt, O. Fuchs, D. Groß, G. Storch, E. Umbach, N. G. Dhere, A. A. Kadam, S. S. Kulkarni, and C. Heske, *Appl. Phys. Lett.* **86**, 062109 (2005).

²⁹Y. Hinuma, F. Oba, Y. Nose, and I. Tanaka, *J. Appl. Phys.* **114**, 043718 (2013).

³⁰T. Minemoto, H. Takakura, and Y. Hamakawa, *Sol. Energy Mater. Sol. Cells* **90**, 3576 (2006).

³¹S. R. Kang, S. W. Shin, D. S. Choi, A. V. Moholkar, J. H. Moon, and J. H. Kim, *Curr. Appl. Phys.* **10**, S473 (2010).

³²Gunawan, W. Septina, S. Ikeda, T. Harada, T. Minegishi, K. Domen, and M. Matsumura, *Chem. Commun.* **50**, 8941 (2014).

³³See supplementary material at <http://dx.doi.org/10.1063/1.4950882> for the surface SEM images of sulfide-coated ZnSnP₂, the GI-XRD profiles of sulfide films, and the details for bandgap evaluation.

³⁴S. Tanuma and T. Kimura, *J. Surf. Anal.* **10**, 163 (2003); available at <https://www.jstage.jst.go.jp/browse/jssa/>.

³⁵D. Hariskos, S. Spiering, and M. Powalla, *Thin Solid Films* **480–481**, 99 (2005).

³⁶C. D. Wagner, W. M. Riggs, L. E. Davis, J. F. Moulder, and G. E. Muilenberg, *Handbook of X-Ray Photoelectron Spectroscopy* (Perkin-Elmer Corporation, Minnesota, 1979), p. 54.

³⁷E. A. Kraut, R. W. Grant, J. R. Waldrop, and S. P. Kowalczyk, *Phys. Rev. Lett.* **44**, 1620 (1980).

³⁸A. Grüneis, G. Kresse, Y. Hinuma, and F. Oba, *Phys. Rev. Lett.* **112**, 096401 (2014).

³⁹Y. Hinuma, A. Grüneis, G. Kresse, and F. Oba, *Phys. Rev. B* **90**, 155405 (2014).